Comparison of perfusion signal acquired by ASL prepared intravoxel incoherent motion (IVIM) MRI and conventional IVIM MRI to unravel the origin of the IVIM-signal

X. Zhang [1], Carson Ingo [2], W.M. Teeuwisse [1], Z. Chen [3], M. J. P. van Osch [1, 4]

[*]Correspondence to: X. Zhang, C. J. Gorter Center for high field MRI, Department of Radiology, Leiden University Medical Center, Albinusdreef 2, 2333ZA Leiden, The Netherlands. E-mail: x.zhang.radi@gmail.com

Institute information:
1. Department of Radiology, C. J. Gorter Center for high field MRI, Leiden University Medical Center, Leiden, The Netherlands
2. Department of Physical Therapy and Human Movement Sciences, Northwestern University, Chicago, IL, USA
3. Center for Biomedical Imaging Research, Department of Biomedical Engineering, Tsinghua University, Beijing, China.
4. Leiden Institute for Brain and Cognition, Leiden University, Leiden, the Netherlands

Running title: ASL-IVIM to unravel the IVIM-signal origin

Key words: intravoxel incoherent motion imaging, IVIM, time encoded pseudo-continuous ASL, te-pCASL, (pseudo-) diffusion coefficient

Abstract

Purpose:

Applications of IVIM in the brain are scarce whereas it has been successfully applied in other organs with promising results. To better understand the cerebral IVIM-signal, the diffusion properties of the arterial blood flow within different parts of the cerebral vascular tree, i.e. different generations of the branching pattern, were isolated and measured by employing an ASL-preparation module before an IVIM read-out.

Methods:

ASL preparation was achieved by T_1-adjusted time-encoded pseudo-continuous ASL (te-pCASL). The IVIM read-out module was achieved by introducing bipolar-gradients immediately after the excitation pulse. The results of ASL-IVIM were compared with those of conventional IVIM to improve our understanding of the signal generation process of IVIM.

Results:

The pseudo-diffusion coefficient D* as calculated from ASL-IVIM data was found to decrease exponentially for PLDs between 883ms and 2176ms, becoming relatively stable for PLDs longer than 2176ms. The fast compartment of the conventional IVIM-experiment shows comparable apparent diffusion values to the ASL-signal with PLDs between 1747ms and 2176ms. At the longest PLDs the observed D*-values ($4.0\pm2.8\times10^{-3}$ mm^2/s) are ~4.5 higher than the slow compartment ($0.90\pm0.05\times10^{-3}$ mm^2/s) of the conventional IVIM-experiment.

Conclusion:

This study showed much more complicated diffusion properties of vascular signal than the conventionally assumed single D* of the perfusion compartment in the two-compartment model of IVIM (bi-exponential behavior).

Key words:

intravoxel incoherent motion imaging, time encoded pseudo-continuous ASL, (pseudo-) diffusion coefficient, IVIM, te-pCASL, ASL-IVIM

Introduction:

Cerebral perfusion is considered an important physiological parameter and perfusion measurements play a more and more important role in the diagnosis of various neurovascular diseases as well as in understanding the mechanisms underlying these diseases (1–3). Perfusion imaging can be achieved by four major magnetic resonance imaging techniques, i.e. dynamic susceptibility contrast MRI (DSC-MRI) (4,5), dynamic contrast enhanced MRI (DCE-MRI) (6), arterial spin labeling (ASL) (7,8) and intravoxel incoherent motion imaging (IVIM) (9,10). Whereas the first three have been widely and successfully implemented in the brain, studies with IVIM are still scarce for cerebral applications. However, attention on IVIM has regained significant interest during the last decade (11–16) and it has been implemented in various organs with promising results (17,18). The fact that application of IVIM in the brain is still lagging behind, could probably be attributed to the small cerebral perfusion fraction, ~5% of the whole brain (12,19), resulting in low SNR.

In the 1980s it was proposed by Le Bihan et al. to measure perfusion by disentangling it from diffusion processes and this approach was dubbed IVIM. The basic assumption of IVIM was that blood flow in the capillaries, known as cerebral perfusion, can be considered as a pseudo-diffusion process due to the random directions within the capillary network. A two compartment IVIM model was proposed to separate the contribution of perfusion from diffusion effects: a slow compartment with diffusion coefficient D of which the signal decays slowly as a function of diffusion weighting (i.e., b-value) due to Gaussian dynamics; and a fast compartment with a perfusion fraction f and pseudo diffusion coefficient D*, where the signal drops much faster as a function of b-value due to pseudo-random capillary

blood flow. A main concern of the validity of this model is that a distribution of velocities as well as non-random orientation could result in a more complex relation than the mono-exponential assumption of the fast compartment as represented by the single D*. Concerns on the validity of the IVIM approach arise also from the reported ratio of gray and white matter CBF (~1.2 with IVIM), which are frequently too low compared to ratios of 2~4 as observed by other techniques (DSC, ASL, O^{15}-H_2O PET) (14,15,20,21). Thus, this approach and especially the model might be too simplified to accurately reflect the underlying blood flow leading to quantification errors for the perfusion parameters. It is important to keep in mind that IVIM provides measures of total blood flow instead of only terminal deposition (22), and that the most stable hemodynamic parameter that can be estimated reflects blood volume instead of blood flow; it provides therefore also information similar to techniques like VASO (19)**.** To better understand the IVIM-signal, it would be advantageous to exclusively measure the diffusion properties of the arterial blood flow and to do this for different sub-parts of the cerebral vascular tree, i.e. different generations of the branching pattern. By employing an ASL-preparation module before an IVIM read-out the signal of the blood pool can be isolated. The goal of the current study is, therefore, to measure the diffusion properties of intra- and extravascular ASL-signal as a function of post-labeling delay (PLD) time, with the PLD acting as a surrogate marker for the level within the vascular tree from which the ASL-signal originates. Moreover, the measured diffusion properties of the ASL-signal were compared to results from a conventional IVIM acquisition.

Methods:

In this study, ASL preparation was achieved by time encoded pseudo-continuous ASL (te-pCASL) which enables ASL-acquisitions at multiple post-labeling delay (PLD) times in a time-efficient manner (23,24). In te-pCASL, the traditional long labeling duration is divided into several (eleven in this study) short blocks (also referred to as 'sub-boli') and the label or control condition of each block is varied according to a Hadamard matrix encoding scheme. After Hadamard decoding, perfusion images can be reconstructed for each block that are similar to a traditional pCASL experiment with the labeling duration equal to the duration of the specific labeling block and a PLD equal to the time between the end of the block and start of readout (see Teeuwisse et al. (24) for detailed information on the ability of this approach to separate signal from different sub-boli). Importantly, the SNR of each reconstructed Hadamard-image is equal to the corresponding traditional pCASL-scan with equal TR and total scan time.

The IVIM read-out module was achieved by introducing bipolar gradients immediately after the 90^{o} excitation pulse of the EPI acquisition, resulting in a flow induced phase shift for moving spins. By increasing the gradient strength of the bipolar gradient, higher effective b-values were obtained:

$$b = \frac{2}{3}\gamma^2 G^2 \delta^3 , \quad (25)$$

γ : *gyromagnetic ratio*;
G : *magnitude of the diffusion gradient pulse*;
δ : *duration of the diffusion gradient pulse.*

Subjects:

Ten healthy participants aged between 20 and 52 years (4 females and 6 males, mean 30 ± 8 years) were scanned on a 3 Tesla Achieva MRI scanner (Philips Healthcare, Best, the Netherlands) using a 32 channel receive head coil. This study was part of a protocol development project as approved by Leiden University Medical Center Committee for Medical Ethics and informed consent was obtained from all subjects.

Acquisition:

For ASL-IVIM, ASL-preparation was based on a T_1 adjusted te-pCASL scheme (order of Hadamard matrix: 12; labeling block durations of 894, 579, 429, 340, 283, 241, 211, 187, 168, 153, 115 ms resulting in a total labeling duration of 3600 ms) which was adjusted to compensate for T_1 decay of label for each specific block based on an assumed T_1 of blood of 1650 ms. Adjustment of block-durations was performed to obtain approximately similar SNR for all PLDs. The interval between the labeling and readout module was 49 ms. Background suppression was included by two spatially selective FOCI pulses at 1925 ms and 3120 ms after the start of labeling (24,26). IVIM readout was achieved by a bipolar gradient (δ=17.5 ms) with increasing values of *G* that corresponded to 8 b-values (0, 0.07, 0.15, 0.6, 3.8, 10.5, 42, 168 s/mm^2 in the phase-encoding (anterior-posterior) direction) and resulted in 8 velocity encoding (VENC) values (∞, 7.5, 5, 2.5, 1, 0.6, 0.3, 0.15 cm/s; $VENC = \sqrt{\frac{2\pi^2}{3b\delta}}$). The following parameters were used: single-shot EPI, 6 slices; slice thickness 7 mm, voxel size 3.75 × 3.75 mm^2, duration of each lobe of bipolar gradient 17.5 ms, total scan duration ~40 min (6 repeats for each b-value), TR 4020 ms, TE 44 ms.

For conventional IVIM, scans were performed with 30 b-values ranging from 0 to 800 s/mm^2 (0, 5, 7, 10, 20, 30, 40, 50, 60, 70, 80, 90, 100, 120, 140, 160, 180, 200, 250, 300, 350, 400, 450, 500, 550, 600, 650, 700, 750, 800 s/mm^2 in the phase-encoding (anterior-

posterior) direction). The following parameters were used: single shot spin echo DWI, 6 slices, slice thickness 7 mm, voxel size 3.75 × 3.75 mm^2, diffusion gradient separation time 34.5 ms, diffusion gradient duration 9.8 ms, total scan duration ~10 min (10 repeats for each b-value).

Post-processing:

All the data were motion corrected and coregistered in SPM, then further analyzed in Matlab, the Mathworks. For ASL-IVIM, the images were Hadamard decoded and the ASL-signal averaged over the whole brain gray matter mask was fitted as a function of b-value to a mono-exponential model:

$$S(PLD, \tau, b)/S_0 = S_{ASL}(PLD, \tau) \bullet \exp(-b \bullet D^*),$$

To further distinguish the intra- and extra vascular contributions to the ASL-signal, an alternative two-compartment, bi-exponential model was implemented following the work of Silva et al. (11) and Wells et al. (27):

$$S(PLD, \tau, b) = S_{ASL\_intra}(PLD, \tau) \bullet \exp(-b \bullet D_{intra}) + S_{ASL\_extra}(PLD, \tau) \bullet \exp(-b \bullet D_{extra})$$

$S_{ASL}(PLD, \tau)$, $S_{ASL\_intra}(PLD, \tau)$, $S_{ASL\_extra}(PLD, \tau)$ are the amplitude of the total ASL signal, and the ASL signal of respectively the intra-vascular and extra-vascular compartment, for a certain PLD and labeling duration (τ) without any diffusion weighting; D_{intra} and D_{extra} are respectively the pseudo-diffusion coefficient of the intra-vascular and extra-vascular compartment. To stabilize the fit of the two-compartment, bi-exponential model initialization values for S_{ASL_intra}, S_{ASL_extra}, D_{intra} and D_{extra} were obtained as the mean fitted value from the bi-exponential model with 100 different initiation values using the Nelder-Mead search method (function fminsearch, MATLAB, The MathWorks). Subsequently, S_{ASL_intra}, S_{ASL_extra}, D_{intra} and D_{extra} were obtained from the bi-exponential fitting using the

initialized values. The whole brain gray matter mask was created by manually thresholding the perfusion weighted images without diffusion weighting. For conventional IVIM, firstly, the signals with b >=200 s/mm^2 were isolated and fitted to a mono-exponential model to estimate the diffusion coefficient D. Secondly, the signals with all b-values were further fitted to a bi-exponential model, while keeping D fixed at the previously estimated value:

$$S(b)/S_0=f\bullet\exp(-b\bullet D^*)+(1-f)\bullet\exp(-b\bullet D),$$

D is the diffusion coefficient of the slow component, D* is the pseudo-diffusion coefficient, f is the perfusion fraction, S_0 is the signal intensity at b=0. IVIM-perfusion signal was isolated by subtracting the mono-exponential signal of the slow-diffusion compartment (D) from the total signal. In order to test whether D_{extra} (averaged over the two longest PLDs, i.e. 2176 and 2755 ms) acquired by ASL-IVIM and D in the slow compartment acquired by conventional IVIM were significantly different from each other, statistical testing was performed using a Student's paired sample t-test. Similarly, it was tested whether the D_{intra} at PLD of 883 ms (where the intravascular ASL-signal reached maximum signal intensity) was different from D^* of conventional IVIM.

Results:

Figure 1 shows as an example of the Hadamard decoded, ASL prepared IVIM images of one subject; these images show in the columns the different sub-boli (each having a specific labeling duration and PLD), whereas the different b-values are displayed in the row-direction. The first column of Figure 1, with a b-value of zero, shows a series of conventional multi-phase ASL images in which the labeled spins are seen to be flowing from the large and medium-sized arteries, further down into the vascular tree, while finally entering the microvasculature and tissue-compartment. Up to a PLD of 1407 ms an approximate constant whole brain-averaged signal intensity can be observed, showing that the T_1-adjusting scheme did perform as expected. However, for the last three PLDs a drop in signal intensity was observed.

For each row it can be appreciated that the overall signal intensity of the ASL-IVIM images are decreasing for higher b-values. For short PLDs, when the ASL-label still resides within the vasculature, little or no signal is observed for high b-values. For longer PLDs, when the inverted spins are entering the brain tissue compartment, ASL-IVIM signal is also preserved for the higher b-values.

Figure 2 shows the average over all 10 subjects the normalized ASL-IVIM signal in whole brain gray matter (the signal of the sub-bolus divided by the corresponding labeling duration to calibrate the ASL-signal for the amount of label as created for that sub-bolus) as a function of PLD showing a clear "Buxton-curve" (28): the ASL signal increases as the inverted spins enter the imaging voxel, whereas for longer PLDs the signal decreases due to longitudinal relaxation and outflow of the inverted spins. Additionally, within the same graph the dependency of the ASL-IVIM signal as a function of b-value is depicted, also

showing an mono-exponential fit of the data (Supporting Figure S1 shows both mono- and bi-exponential fits to the ASL signal as a function of b-values for each individual PLD). For the shortest PLD no fit could be made, since insufficient amount of label had entered the imaging slice leaving too little signal for even the lowest b-values.

Figure 3 shows for the different PLDs, averaged across all subjects, the pseudo-diffusion coefficient D* (a) and the natural logarithm of D* (b) as obtained from the mono-exponential fit to the ASL-IVIM data, D_{intra} (c), the natural logarithm of D_{intra} (d), D_{extra} (e) and the natural logarithm of D_{extra} (f) as obtained from the bi-exponential fit. The observed D*-values at the longest PLDs was found to be $4.0 \pm 2.8 \times 10^{-3}$ mm^2/s using mono-exponential model, and D_{extra} was $1.9 \pm 1.4 \times 10^{-3}$ mm^2/s using the bi-exponential model. The quantified values from conventional IVIM were found to be: f = 0.10 ± 0.02, D = 0.90 ± 0.05 (10^{-3} mm^2/s), and D* = 11.8 ± 1.7 (10^{-3} mm^2/s). D* at the longest PLDs (averaged over the two longest PLDs, i.e. 2176 and 2755 ms) of ASL-IVIM was statistically significant different from the slow compartment (D) of conventional IVIM (p=0.007), similarly a significant difference was found between extravascular D at the longest PLDs and the slow compartment D of conventional IVIM (p=0.045). Moreover, the intravascular D at the PLD of 882 ms (when the intravascular ASL-signal reached maximum signal intensity, D_{intra}=10.7 ± 11.5 mm^2/s) was much higher than the fast compartment D* ($11.8 \pm 1.7 \times 10^{-3}$ mm^2/s) of conventional IVIM (p=0.016).

Figure 4 shows the time-course of the total ASL signal as well as the intra-vascular and extra-vascular signals as obtained from the two compartment model. At short PLDs ASL-signal is predominantly intravascular, whereas for PLDs>1407 ms the majority of signal is

from the extra-vascular compartment. Interestingly, even at the longest PLDs a small amount of ASL-signal originates from the intra-vascular compartment.

Figure 5 shows the fitted, normalized signal using the mono-exponential model (a), the intra-vascular signal (b) and extra-vascular signal (c) using the two-compartment bi-exponential model acquired by ASL-IVIM as a function of b-values for different PLDs as well as the fast and slow compartment of conventional IVIM. The fast compartment of the conventional IVIM-experiment shows comparable apparent diffusion values to the ASL-signal with a PLD between 1747 ms and 2176 ms using mono-exponential model and with a PLD between 1407 ms and 1747 ms in the extra-vascular compartment using bi-exponential model. .

Discussion:

In this study, the diffusion properties of the arterial blood compartment were measured by monitoring the passage of the inverted blood in time by means of an ASL preparation. By using a te-pCASL-preparation module before the IVIM readout, different parts of the vascular tree are sampled by effectively creating a multi-PLDs ASL dataset in a time-efficient manner. To better understand the signal generation of conventional IVIM, the results of ASL prepared IVIM were compared with results obtained by conventional IVIM. Using mono-exponential fitting for the ASL-IVIM, D* as calculated from ASL-IVIM data was found to be highly dependent on the PLD. D* at very short PLDs (smaller than 600 ms) could not be fitted due to the low amount of signal present for even the lowest b-values. Very high D*-values of 8~13 mm^2/s were observed for PLDs of 672~883 ms, which can be explained by ASL-signal being present in larger arteries for these short PLDs. For longer PLDs the labeled blood travels further down the vascular tree with D* decreasing exponentially for 883 ms<PLD<2176 ms (Figure 3), suggesting that more and more of the ASL-signal originates from the microvasculature or even originates from the extravascular compartment of the brain tissue. Finally, for PLD> 2176 ms the D* remains relatively stable suggesting that the inverted spins have extravasated into the extravascular compartment and therefore reflects diffusion in tissue. However, the fact that at the longest PLDs the observed D*-values ($4.0\pm2.8 \times 10^{-3}$ mm^2/s) are still a factor ~4.5 higher than the diffusion coefficient of the slow compartment ($0.90\pm0.05 \times 10^{-3}$ mm^2/s) of the conventional IVIM-experiment, seems to contradict this explanation. This might indicate that the extravascular compartment into which the ASL-signal accumulates, is only a sub-

part of the compartment that is probed by the slowly-diffusing signal of the IVIM experiment.

A two-compartment, bi-exponential model was also performed to further distinguish the contributions from the intra-vascular and extra-vascular compartments. Similar results were found as from the mono-exponential model, while the bi-exponential fitting describes the ASL signal as a function of b-value more accurately (Supplementary Figure 1). Intra-vascular D (D_{intra}) and extra-vascular D (D_{extra}) were highly dependent on PLDs, reaching a plateau at long PLDs. The averaged D_{extra} at long PLDs (PLD>2176 ms) was found to be ~1.9±1.4×10^{-3} mm^2/s, which is two times lower than the D* using the mono-exponential model (~4.0±2.8×10^{-3} mm^2/s). This lower value could be explained by the fact that the mono-exponential model is indeed a too simplified approach, resulting in a weighted average between diffusion properties of the intra- and extravascular ASL-signal. But the D_{extra} is still two times higher than the diffusion coefficient of the slow compartment (0.90±0.05 × 10^{-3} mm^2/s) of the conventional IVIM-experiment, which might again indicate that the ASL-signal does not exchange with the complete extravascular compartment, but with only a sub-part.

The signal from the fast compartment as detected by the conventional IVIM scan shows an intermediate D*-value corresponding to the ASL-IVIM signal for a PLD between 1750~2176 ms (see figure 5.a). The root mean squared displacement (RMSD) of ASL-IVIM calculated as $\sqrt{2*D*\delta}$ is found to be ~12 microns, while RMSD calculated as $\sqrt{2*D*(\Delta-\frac{\delta}{3})}$ for conventional IVIM is found to be ~7 microns in the slow compartment and ~27 microns in the fast compartment. This might indicate that the IVIM

signal does not only originate from the microvasculature, but also reflects a considerable amount of vascular signal, considering the fast decrease of D* as observed for PLDs smaller than 2176 ms.

A similar approach referred to as DW-ASL that employed an ASL-preparation module followed by a spin-echo diffusion weighted imaging module was proposed by Silva et al. (11) and subsequently applied by St. Lawrence et al. (29) and Wang et al. (30). Whereas, only Wang et al. provided a direct comparison between ASL-IVIM and conventional IVIM data, this was not performed at as many PLDs as this study and did therefore provide little information on the origin of the IVIM-signal within the vascular tree. These studies were primarily aimed at measuring the exchange of arterial spin labeled water from the intra- to the extra-vascular compartment and thus to measure the exchange rate of water across the blood-brain-barrier. A similar approach was adopted by Duong et al. (31), who instead of using the arterial blood as endogenous tracer, injected perfluorocarbon 19F as an intra-vascular tracer to measure the diffusion properties of the arterial and venous blood volume compartments in rats. Our study instead aimed to investigate the origin of conventional IVIM signal by investigating the ASL signal as a function of b-value while the blood traverses through the vascular tree. Due to the use of time-encoded pCASL the diffusion properties of the ASL-signal could be obtained in a highly time-efficient manner for many different PLDs. When we compare our results for PLDs<1747 ms with the results of St. Lawrence's study in which the perfusion signal was measured as a function of b-value for only 4 PLDs ranging from 900 ms to 1800 ms, a good agreement can be observed. In our study, we also measured with longer PLDs showing that conventional IVIM measures an intermediate D*-value as compared to ASL-IVIM.

The mean whole brain perfusion signal was rather stable for PLDs smaller than 1750 ms, which can be attributed to the T_1-adjusted time-encoded labeling scheme that was designed to preserve signal-to-noise ratio (SNR) by compensating for loss of signal due to T_1 relaxation by increasing the sub-bolus labeling duration. For the reconstructed ASL-images with the three longest PLD a drop of signal intensity can be observed what can be explained by the fact that the ASL signal will relax with the T_1 of tissue for these longer PLDs since some of the inverted spins will have exchanged into the tissue (compare the T_1 of 1200 ms in gray matter with the blood T_1 of 1650 ms employed in the design of the T_1-adjusting scheme).

A limitation of the current study is that all gradients for the IVIM readout module were along a single direction (the phase-encoding direction), which may underestimate the complexity of the blood flow in capillaries and also the directional flow for shorter PLDs. A recent study by Wells et al. (27) applied motion sensitizing gradients in three directions in an ASL prepared IVIM technique to investigate cerebral microvascular flow patterns in rats, showing that ASL-IVIM has the ability to capture important information on the architecture of the microvascular bed. Including more than one direction for the IVIM gradients would improve the information content of the ASL-IVIM scans, but it would also increase the scan duration significantly. It is important to note that in this study, the direction of the IVIM gradient was identical for both the ASL-IVIM and the conventional IVIM experiments, resulting in a fair comparison. With the current ASL preparation that allows time-efficient acquisition of multi-phase ASL signal, the amount of the labeled blood in the different levels of cerebral vascular tree cannot be explicitly quantified. With the more complete, second model an estimate was obtained for the intra- and extravascular

components of the ASL-signal, but by combining the current approach with a TRUST-module to measure the T_2 of the ASL-signal (32,33), even more information on the spin-compartment could potentially be obtained.

Conclusion:

In this study, ASL-IVIM was successfully employed to study the diffusion characteristics of the arterial blood flow. This study showed much more complicated diffusion properties of vascular signal than the conventionally assumed single compartment, mono-exponential behavior in IVIM.

Acknowledgements:

This research is supported by the Dutch Technology Foundation STW, applied science division of NWO and the Technology Program of the Ministry of Economic Affairs.

Reference:

1. Christensen S, Mouridsen K, Wu O, Hjort N, Karstoft H, Thomalla G, Rother J, Fiehler J, Kucinski T, Ostergaard L. Comparison of 10 Perfusion MRI Parameters in 97 Sub-6-Hour Stroke Patients Using Voxel-Based Receiver Operating Characteristics Analysis. Stroke 2009;40:2055–2061. doi: 10.1161/STROKEAHA.108.546069.
2. Provenzale JM, Shah K, Patel U, McCrory DC. Systematic review of CT and MR perfusion imaging for assessment of acute cerebrovascular disease. AJNR Am. J. Neuroradiol. [Internet] 2008;29:1476–1482. doi: 10.3174/ajnr.A1161.
3. Alsop DC, Detre J a, Golay X, et al. Recommended implementation of arterial spin-labeled perfusion MRI for clinical applications: A consensus of the ISMRM perfusion study group and the European consortium for ASL in dementia. Magn. Reson. Med. [Internet] 2014;0. doi: 10.1002/mrm.25197.
4. KETY SS. Quantitative determination of cerebral blood flow in man. Methods Med. Res. [Internet] 1948;1:204–17.
5. Villringer A, Rosen BR, Belliveau JW, Ackerman JL, Lauffer RB, Buxton RB, Chao YS, Wedeen VJ, Brady TJ. Dynamic imaging with lanthanide chelates in normal brain: contrast due to magnetic susceptibility effects. Magn. Reson. Med. [Internet] 1988;6:164–74.
6. O'Connor JPB, Tofts PS, Miles KA, Parkes LM, Thompson G, Jackson A. Dynamic contrast-enhanced imaging techniques: CT and MRI. Br. J. Radiol. [Internet] 2011;84:S112–S120. doi: 10.1259/bjr/55166688.
7. Detre JA, Leigh JS, Williams DS, Koretsky AP. Perfusion imaging. Magn. Reson. Med. [Internet] 1992;23:37–45. doi: 10.1002/mrm.1910230106.
8. Williams DS, Detre JA, Leigh JS, Koretsky AP. Magnetic resonance imaging of perfusion using spin inversion of arterial water. Proc. Natl. Acad. Sci. U. S. A. [Internet] 1992;89:212–6.
9. Le Bihan D. Intravoxel incoherent motion imaging using steady-state free precession. Magn. Reson. Med. [Internet] 1988;7:346–351. doi: 10.1002/mrm.1910070312.
10. Bihan D Le, Turner R. The capillary network: a link between ivim and classical perfusion. Magn. Reson. Med. 1992;27:171–178. doi: 10.1002/mrm.1910270116.
11. Silva AC, Williams DS, Koretsky AP. Evidence for the exchange of arterial spin-labeled water with tissue water in rat brain from diffusion-sensitized measurements of perfusion. Magn. Reson. Med. [Internet] 1997;38:232–237. doi: 10.1002/mrm.1910380211.
12. Federau C, Eth DP, Maeder P, Brien KO, Browaeys P. Quantitative Measurement of Brain Perfusion with Intravoxel. 2012;265.
13. Federau C, Meuli R, O'Brien K, Maeder P, Hagmann P. Perfusion measurement in brain gliomas with intravoxel incoherent motion MRI. AJNR. Am. J. Neuroradiol. [Internet] 2014;35:256–62. doi: 10.3174/ajnr.A3686.
14. Federau C, O'Brien K, Meuli R, Hagmann P, Maeder P. Measuring brain perfusion with intravoxel incoherent motion (IVIM): initial clinical experience. J. Magn. Reson. Imaging [Internet] 2014;39:624–32. doi: 10.1002/jmri.24195.
15. Federau C, Sumer S, Becce F, Maeder P, O'Brien K, Meuli R, Wintermark M. Intravoxel incoherent motion perfusion imaging in acute stroke: initial clinical experience. Neuroradiology [Internet] 2014;56:629–35. doi: 10.1007/s00234-014-1370-y.

16. Rydhög AS, van Osch MJP, Lindgren E, Nilsson M, Lätt J, Ståhlberg F, Wirestam R, Knutsson L. Intravoxel incoherent motion (IVIM) imaging at different magnetic field strengths: what is feasible? Magn. Reson. Imaging [Internet] 2014;32:1247–58. doi: 10.1016/j.mri.2014.07.013.
17. Luciani A, Vignaud A, Cavet M, Tran Van Nhieu J, Mallat A, Ruel L, Laurent A, Deux J-F, Brugieres P, Rahmouni A. Liver Cirrhosis: Intravoxel Incoherent Motion MR Imaging—Pilot Study. Radiology [Internet] 2008;249:891–899. doi: 10.1148/radiol.2493080080.
18. Yamada I, Aung W, Himeno Y, Nakagawa T, Shibuya H. Diffusion Coefficients in Abdominal Organs and Hepatic Lesions: Evaluation with Intravoxel Incoherent Motion Echo-planar MR Imaging. Radiology [Internet] 1999;210:617–623. doi: 10.1148/radiology.210.3.r99fe17617.
19. Lu H, Law M, Johnson G, Ge Y, van Zijl PCM, Helpern JA. Novel approach to the measurement of absolute cerebral blood volume using vascular-space-occupancy magnetic resonance imaging. Magn. Reson. Med. [Internet] 2005;54:1403–1411. doi: 10.1002/mrm.20705.
20. Wang L, Lin J, Liu K, Chen C, Liu H, Lv P, Fu C, Zeng M. Intravoxel incoherent motion diffusion-weighted MR imaging in differentiation of lung cancer from obstructive lung consolidation: comparison and correlation with pharmacokinetic analysis from dynamic contrast-enhanced MR imaging. Eur. Radiol. [Internet] 2014;24:1914–22. doi: 10.1007/s00330-014-3176-z.
21. Wu W-C, Chen Y-F, Tseng H-M, Yang S-C, My P-C. Caveat of measuring perfusion indexes using intravoxel incoherent motion magnetic resonance imaging in the human brain. Eur. Radiol. [Internet] 2015. doi: 10.1007/s00330-015-3655-x.
22. Henkelman RM. Does IVIM measure classical perfusion? Magn. Reson. Med. [Internet] 2005;16:470–475. doi: 10.1002/mrm.1910160313.
23. Gunther M. Highly efficient accelerated acquisition of perfusion inflow series by cycled arterial spin labeling. In: Proceedings of the 15th Annual Meeting of ISMRM. Berlin, Germany; 2007.
24. Teeuwisse WM, Schmid S, Ghariq E, Veer IM, van Osch MJ. Time-encoded pseudocontinuous arterial spin labeling: Basic properties and timing strategies for human applications. Magn Reson Med [Internet] 2014. doi: 10.1002/mrm.25083.
25. Freidlin RZ, Kakareka JW, Pohida TJ, Komlosh ME, Basser PJ. A spin echo sequence with a single-sided bipolar diffusion gradient pulse to obtain snapshot diffusion weighted images in moving media. J. Magn. Reson. [Internet] 2012;221:24–31. doi: 10.1016/j.jmr.2012.04.010.
26. Ordidge RJ, Wylezinska M, Hugg JW, Butterworth E, Franconi F. Frequency offset corrected inversion (FOCI) pulses for use in localized spectroscopy. Magn. Reson. Med. [Internet] 1996;36:562–566. doi: 10.1002/mrm.1910360410.
27. Wells JA, Thomas DL, Saga T, Kershaw J, Aoki I. MRI of cerebral micro-vascular flow patterns : A multi-direction diffusion-weighted ASL approach. 2016. doi: 10.1177/0271678X16660985.
28. Buxton RB, Frank LR, Wong EC, Siewert B, Warach S, Edelman RR. A general kinetic model for quantitative perfusion imaging with arterial spin labeling. Magn Reson Med [Internet] 1998;40:383–396.

29. St Lawrence KS, Owen D, Wang DJJ. A two-stage approach for measuring vascular water exchange and arterial transit time by diffusion-weighted perfusion MRI. Magn. Reson. Med. [Internet] 2012;67:1275–84. doi: 10.1002/mrm.23104.
30. Wang J, Fernández-Seara MA, Wang S, Lawrence KSS. When Perfusion Meets Diffusion: *in vivo* Measurement of Water Permeability in Human Brain. J. Cereb. Blood Flow Metab. [Internet] 2007;27:839–849. doi: 10.1038/sj.jcbfm.9600398.
31. Duong TQ, Kim SG. In vivo MR measurements of regional arterial and venous blood volume fractions in intact rat brain. Magn Reson Med 2000;43:393–402. doi: 10.1002/(SICI)1522-2594(200003)43:3<393::AID-MRM11>3.0.CO;2-K.
32. Schmid S, Teeuwisse WM, Lu H, van Osch MJP. Time-efficient determination of spin compartments by time-encoded pCASL T2-relaxation-under-spin-tagging and its application in hemodynamic characterization of the cerebral border zones. Neuroimage [Internet] 2015;123:72–79. doi: 10.1016/j.neuroimage.2015.08.025.
33. Lu H, Ge Y. Quantitative evaluation of oxygenation in venous vessels using T2-Relaxation-Under-Spin-Tagging MRI. Magn. Reson. Med. [Internet] 2008;60:357–363. doi: 10.1002/mrm.21627.

Labeling duration (ms)	PLD (ms)	Perfusion weighted images							
115	49	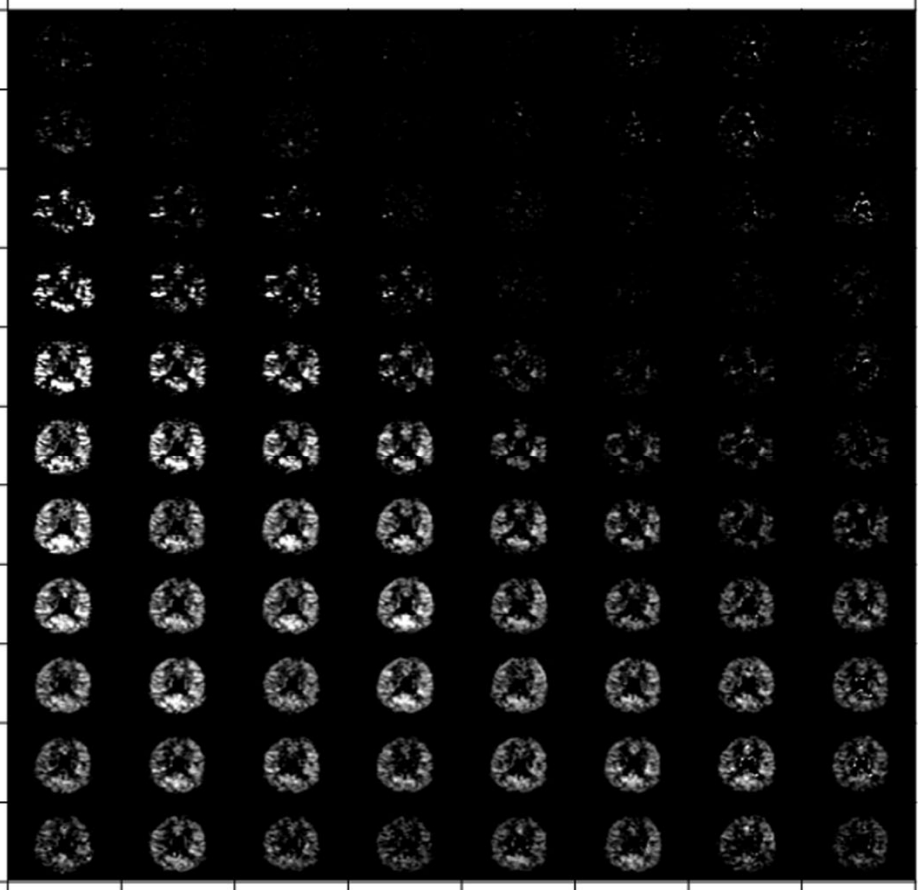							
153	164								
168	317								
187	485								
211	672								
241	883								
283	1124								
340	1407								
429	1747								
579	2176								
894	2755								
		0	0.07	0.15	0.6	3.8	10.5	42	168
		b-values (s/mm^2)							

Figure 1: Hadamard-decoded ASL prepared IVIM images for different PLDs (in rows) and different b-values (in columns).

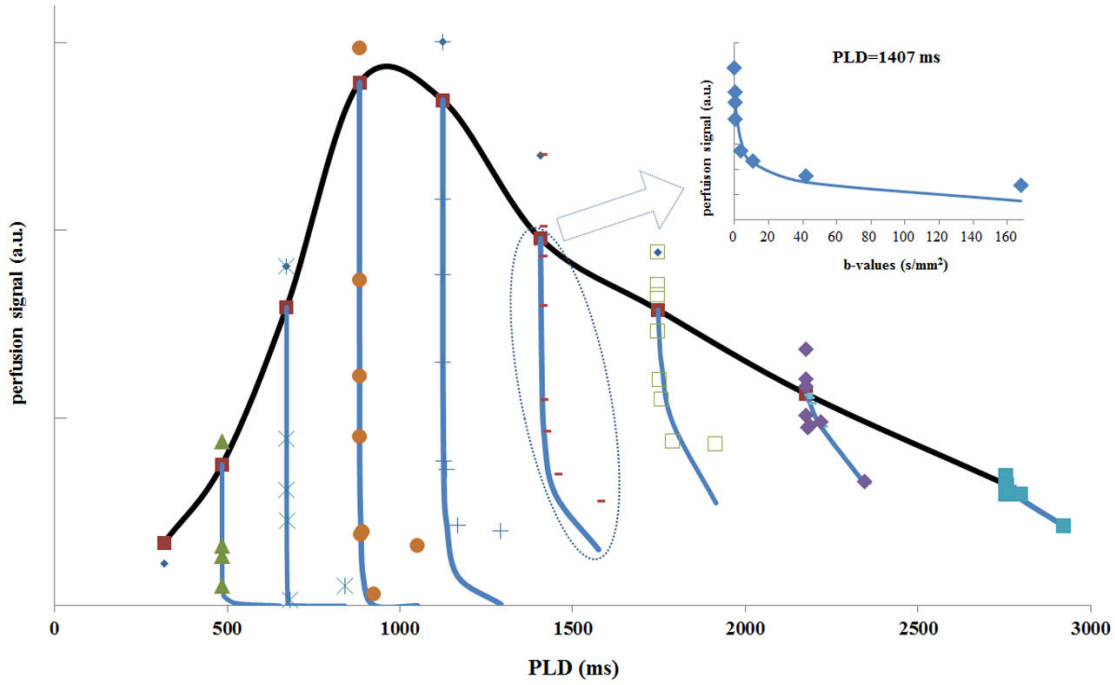

Figure 2: Time-courses of normalized perfusion-signal (Hadamard-decoded ASL-IVIM signal divided by labeling duration) in gray matter as a function of post-labeling delay (PLD) as depicted by the black curve with red square markers, a smooth interpolation was performed to improve the visualization. For each PLD the ASL-signal for different b-values has been plotted on top (blue). A zoomed version of the ASL-signal as a function of b-value is shown in the top-right corner.

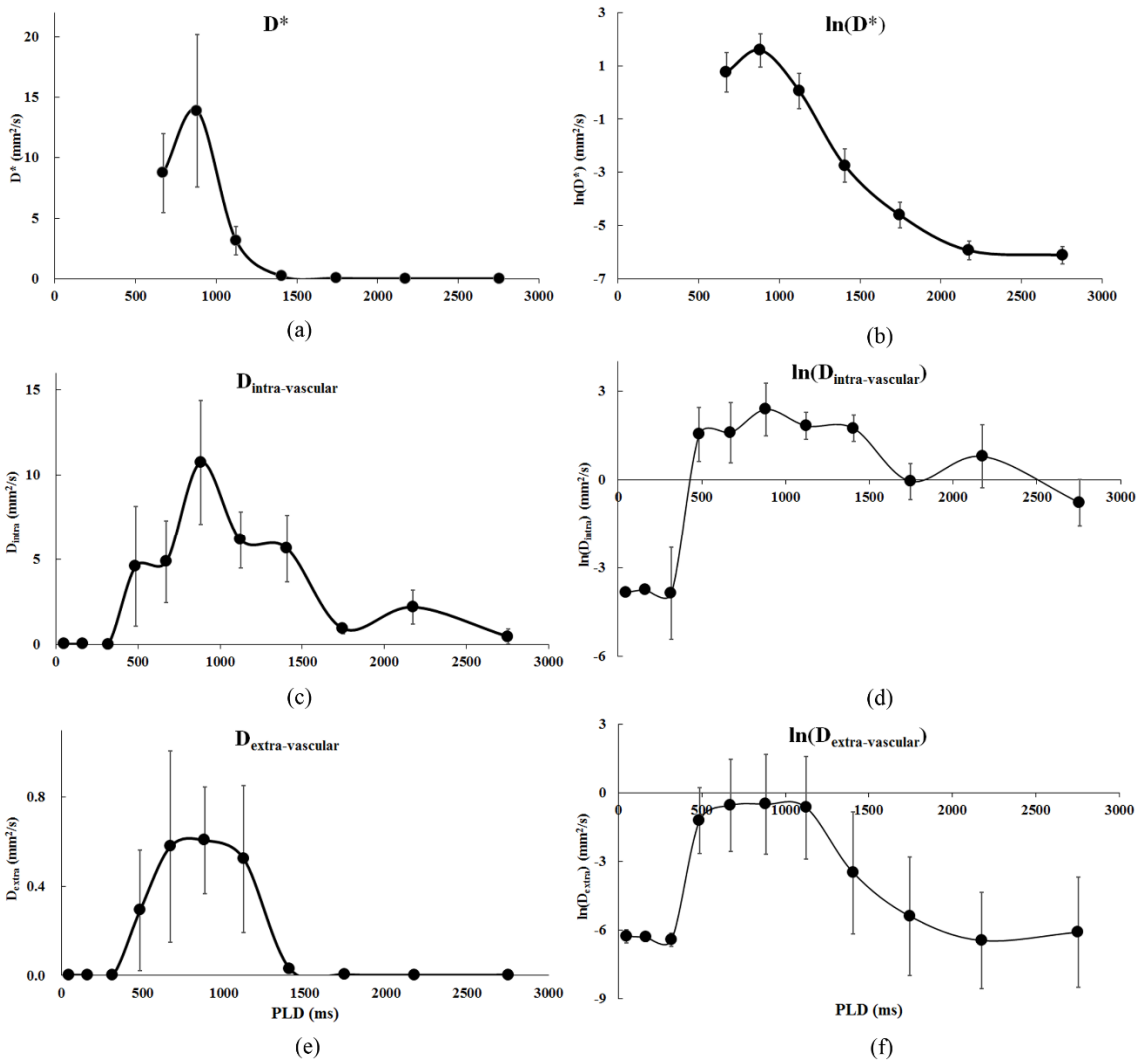

Figure 3: For different PLDs, the pseudo-diffusion coefficient D* (a) and natural logarithm of D* (b) as obtained from the mono-exponential fit to the ASL-IVIM data, D_{intra} (c), natural logarithm of D_{intra} (d), D_{extra} (e) and natural logarithm of D_{extra} (f) as obtained from the bi-exponential fit. The error bars represent the standard-error of the mean values among the subjects.

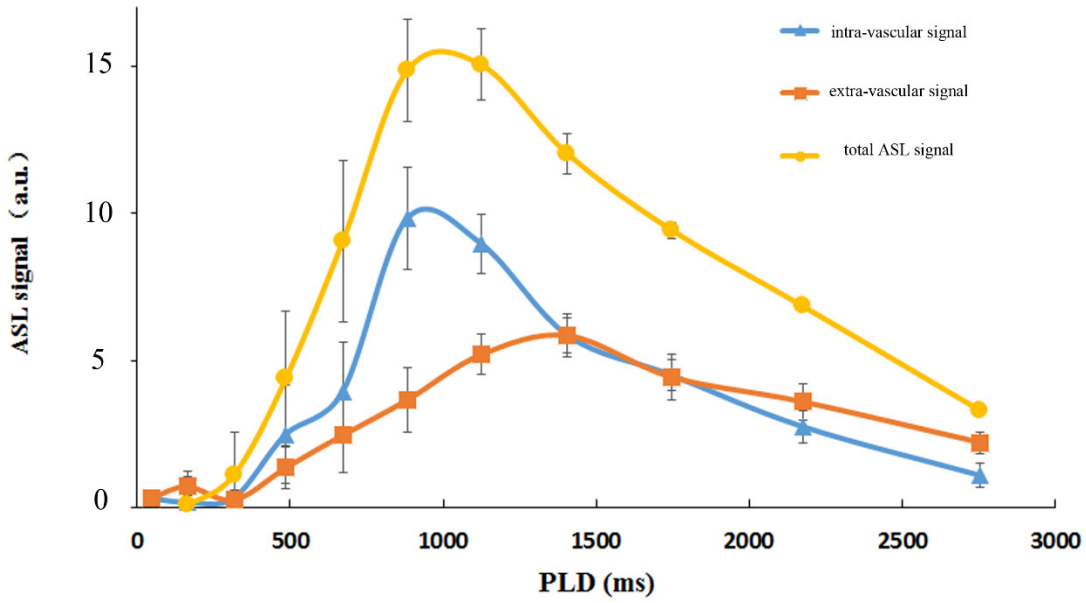

Figure 4: Time-course of the total ASL signal as well as the intra-vascular and extra-vascular signal. The error bars represent the standard-error of the mean values among the subjects.

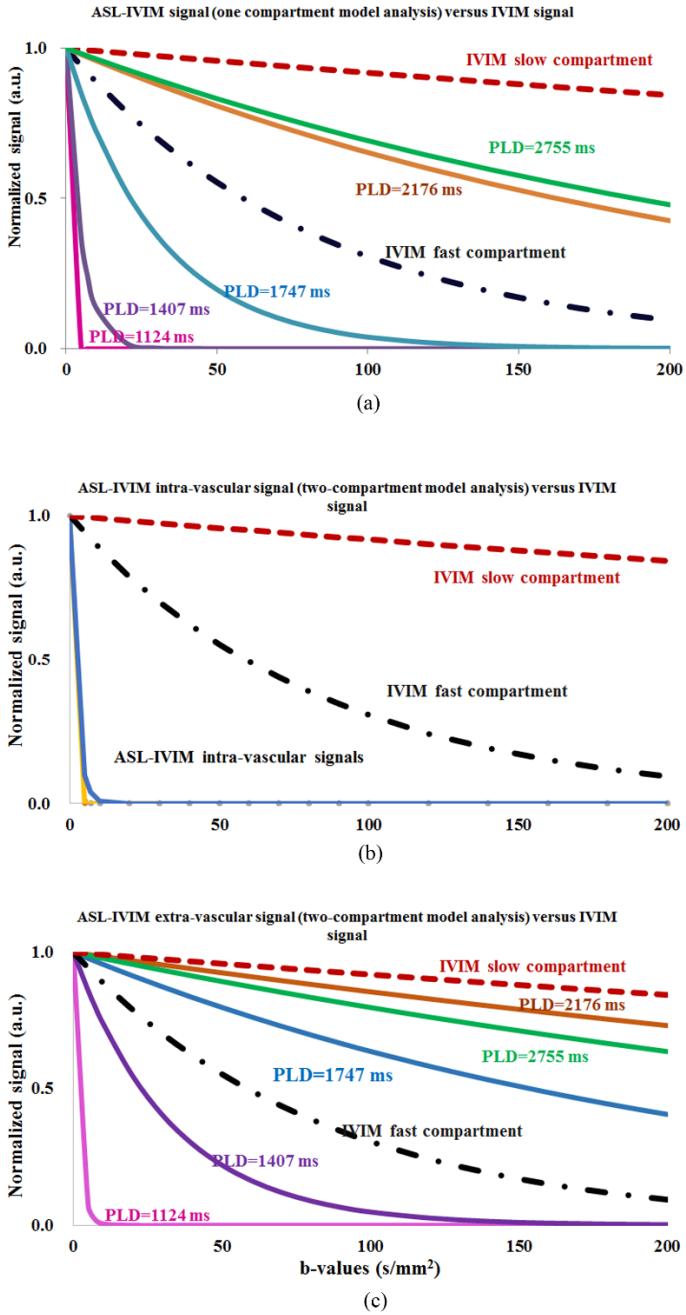

Figure 5: Fitted and Normalized signal using the mono-exponential model (a), the intra-vascular signal (b) and extra-vascular signal (c) using the two-compartment bi-exponential model acquired by ASL-IVIM as a function of b-values for different PLDs as well as the fast and slow compartment of conventional IVIM.

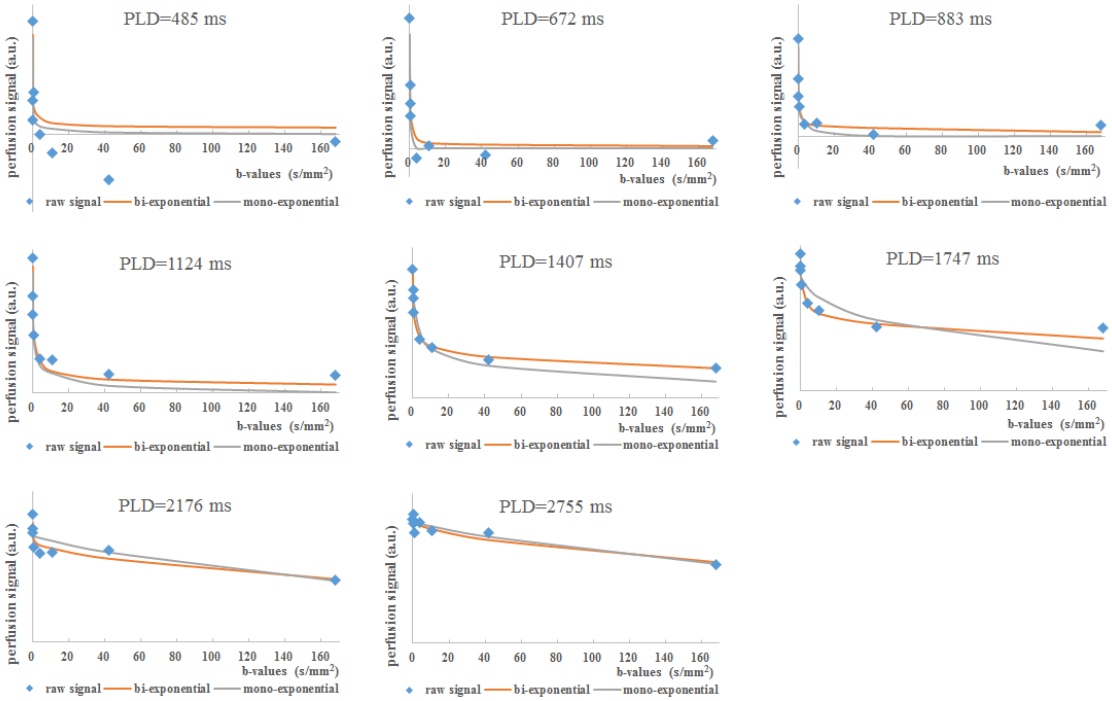

Supporting Figure S1: Data fitting of the ASL signal (blue) as a function of b-values at each individual PLDs using both mono-exponential (purple) and bi-exponential (red) model.